8B.3 GROUND TRUTH VERIFICATION OF THE HAIL QUADRATURE PARAMETER (HQP)

Patrick C. Kennedy*, T.K. Depue[1], R. Cifelli[1], D. Barjenbruch[2], C. Gimmestad[2], D.A. Brunkow[1], and S.A. Rutledge[1]
[1]Colorado State University, Fort Collins, Colorado
[2]National Weather Service Forecast Office, Boulder, Colorado

1. INTRODUCTION

The accurate radar identification of hail, particularly hail capable of inflicting damage, is an important issue in operational meteorology. Differential reflectivity (Z_{dr}; 10 Log_{10} (Z_{hh}/Z_{vv}); first subscript is receive polarization, second is transmit polarization) data collected by dual linear polarization radars can detect the inherent mean shape and orientation differences between larger raindrops (with preferentially oblate shapes), and hailstones (with generally random orientations). An application of this principle is the Hail Differential Reflectivity (HDR) parameter presented by Aydin et al. (1986):

$$HDR = Z_{hh} - f(Z_{dr}) \qquad (1)$$

$$f(Z_{dr}) = \begin{cases} 27 & Z_{dr} = 0 \text{ dB} \\ (19 * Z_{dr}) + 27 & 0 < Z_{dr} = 1.74 \\ 60 & Z_{dr} > 1.74 \end{cases}$$

The prescribed function of Z_{dr} in eq. 1 represents the upper limit of the rain region in Z_{hh} vs. Z_{dr} space. Due to their tumbling motions, the Z_{hh} and Z_{vv} returns from hailstones will tend to be equal; yielding a near 0 dB Z_{dr} value. Near 0 dB Z_{dr}'s will minimize $f(Z_{dr})$, causing hail echoes to have large positive HDR's (i.e., large Z_{hh} and low Z_{dr}). However, once Z_{dr} values in hail decrease to 0 dB, HDR becomes a simple offset from reflectivity.

An additional hail characteristic that may be measured by polarimetric radar is Linear Depolarization Ratio (LDR; 10 Log_{10} (Z_{vh}/Z_{hh})). Qualitatively, the depolarization level of the backscattered signal is increased when non-spherically shaped scatterers are oriented with their major axes out of the polarization plane of the illuminating radar pulse. The LDR increases due to these shape and orientation effects are enhanced when the bulk refractive index of the particles is large. Thus, high density and / or wet, irregularly shaped hailstones can be expected to generate large (>~ -20 dB at S-Band) LDR values.

The Hail Quadrature Parameter (HQP, Kennedy et al., 2001) was devised to combine HDR and LDR measurements. HQP is the magnitude of a two-dimensional vector whose components are HDR and LDR (Fig. 1). The HQP domain (5 < HDR < 50 dB; -25 < LDR < -10 dB) has been chosen to include the expected range of hail values at radar wavelengths of ~ 10 cm. Finally, the HQP axes in this domain are scaled from 0 to 1 so that the HQP of the most distant point (HDR=50, LDR=-10) is the square root of 2.

This vector formulation is based on the assumption that both significant HDR magnitudes and enhanced depolarization levels might individually be associated with large and / or damaging hail. Existing research results provide support for this idea: It has been suggested that hailfall kinetic energy might be maximized in areas where particularly high reflectivity values are associated with low Z_{dr}'s (Aydin et al., 1986, Husson and Pointin, 1989); i.e. when HDR's are large. Also, Knight (1986) found a tendency for hailstone axis ratios to decrease with increasing diameter. To a first approximation, the less spherical shapes of these larger hailstones would promote greater depolarization levels.

The primary goal of this paper is to examine the relationships between HQP, HDR and the observed hailfall characteristics as determined by data gathered in post-storm surveys. Additional insights into the fundamental behavior of the radar variables upon which HDR and HQP are based were obtained from numerical scattering model calculations.

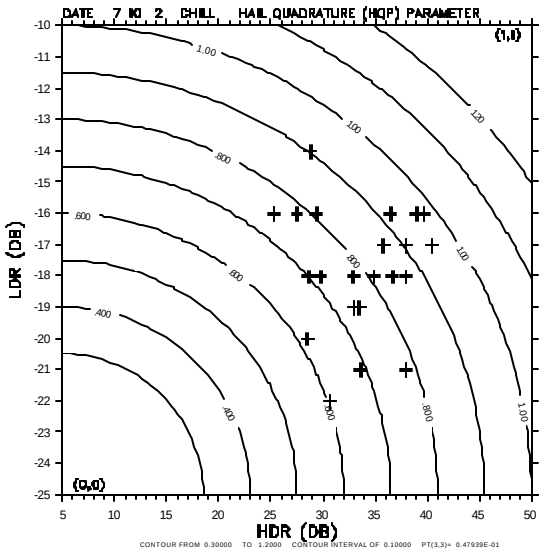

Figure 1: Graphical presentation of HQP as the magnitude of a vector composed of normalized HDR and LDR components. Plus symbols are range gate data points from a damage survey point in The Pinery hailstorm of 10 July 2002.

*Corresponding author address: Patrick C. Kennedy, CSU-CHILL Radar Facility, 30750 Weld Co. Rd. 45, Greeley, CO 80631; e-mail: pat@chill.colostate.edu

2. ELECTROMAGNETIC SCATTERING CALCULATIONS

The response of HQP to variations in the physical characteristics of hailstones was calculated using the transition matrix (T-matrix) method (Waterman, 1969). Fundamentally, for prescribed radar observational conditions (wavelength, elevation angle and particle temperature), this model calculates Z_{hh}, Z_{dr}, and LDR values as a function of the size, aspect ratio, orientation, and refractive index properties of the illuminated particle. To simulate melting effects, an external water coating on the hailstone is permitted. These calculations also include Mie resonance effects.

As expected, the aspect ratio and orientation of the modeled ice particles were of fundamental importance. In general, both decreasing the hailstone axis ratio (through a range of 0.95 to 0.60), and increasing the standard deviation of a Gaussian distribution of canting angles (from 25 to 75°) increased the depolarization levels. This broadening of the canting angle distribution also reduced the Z_{dr} values. (The basic hailstone orientation was taken to have the major axis in the horizontal plane). The use of a random distribution of hailstone orientations caused Z_{dr} to be identically 0 dB. Thus, in a most general sense, LDR still contains some hailstone shape information when Z_{dr} approaches 0 dB due to large orientation fluctuations.

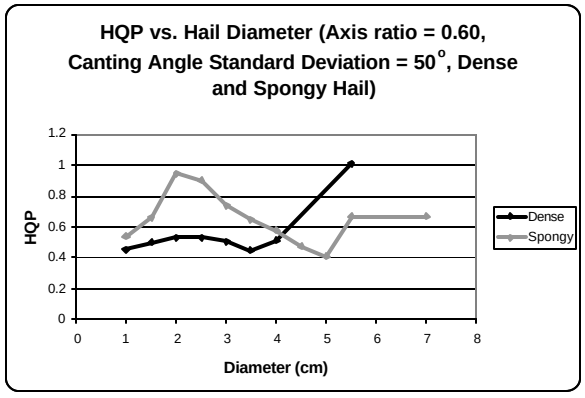

Figure 2: Calculated HQP as a function of hailstone diameter for dense (solid ice) and spongy (ice and water) hailstone composition. (See text for details).

However, these basic patterns are impacted by Mie resonance effects. Figure 2 shows the modeled HQP values for a series of monodisperse hail diameters for a radar wavelength of 11 cm. In this figure, the axis ratio and standard deviation of the canting angle distribution are fixed at 0.6 and 50° respectively. Separate curves are drawn for the cases of hailstones composed of water coated solid (.9 gm cm-3) and spongy (40% water component) ice. In both cases, and most particularly in the spongy case, the idealized positive correlation between hail diameter and HQP suffers occasional reversals at diameters above 2 – 3 cm. At these points Mie resonances (especially local Z_{hh} and LDR decreases and Z_{dr} increases) impact HQP. Similar reversals are found at particular diameters in the dry hail (no water coating) runs (not shown).

These modeling results suggest that HQP values should be interpreted with caution since a unique relationship with hail diameter is not guaranteed to exist. It is expected, however, that natural hailfalls are rarely monodisperse on the size scale of a radar pulse volume. The presence of some hailstones with sizes outside of the critical Mie diameters would tend out to smooth out the local HQP fluctuations seen in Fig. 2. Field project data were used to evaluate the performance of the HQP and HDR hail parameters under naturally occurring conditions.

3. THE COMET 2002 PROJECT

During June – September 2002 a pilot project was conducted at the CSU-CHILL radar facility. This project was supported by the COMET (Cooperative Program for Operational Meteorology, Education, and Training) office to explore the ability of polarimetric radar data to improve the operational characterization of hail and the estimation of rainfall. (See also Cifelli et al. in this preprint volume). The polarimetric radar data were collected by the 11 cm wavelength CSU-CHILL system, located near Greeley, Colorado. During COMET project operations, the radar was operated with the transmitted polarization state alternating between horizontal and vertical. Signal moments were calculated using 128 such samples (64 H and 64 V); the standard azimuthal scan rate was 6 $^{o}s^{-1}$. To support regional precipitation mapping, 360 degree PPI scans were generally done at elevation angles between 0.5° and 3°. Volume scan cycle times were typically 5-6 minutes.

For the purposes of this analysis, a Cressman weighting scheme was used to interpolate the basic radar gate data to a Cartesian grid point network on a selected PPI sweep surface. (The lowest (0.5°) sweep was preferred unless the area of interest was contaminated by blockage, etc.) The interpolation radius of influence was ~ 0.7 times the azimuthal beam separation at the range of the hail signature of interest. Basic quality thresholds were applied to the input data in an effort to remove noisy or otherwise suspect data from the interpolations.

HDR and HQP values were computed from the interpolated Z_{hh}, Z_{dr}, and LDR values generated by each of the input PPI sweeps. To generate a map of the radar-indicated hail swath, the maximum HQP value realized at each grid point over the lifetime of the event was retained.

To obtain hail verification data, post storm survey trips were made to approximately 10 different HQP swaths. Efforts were made to contact local individuals who had directly experienced the hail event. To estimate the hailstone diameters, such witnesses were asked to select the most representative member of a collection of wooden

calibration spheres. They were also asked a set of standard questions regarding the hail's apparent density, degree of ground coverage, damage effects, etc. The hail observer's location was documented through the use of a hand-held GPS unit.

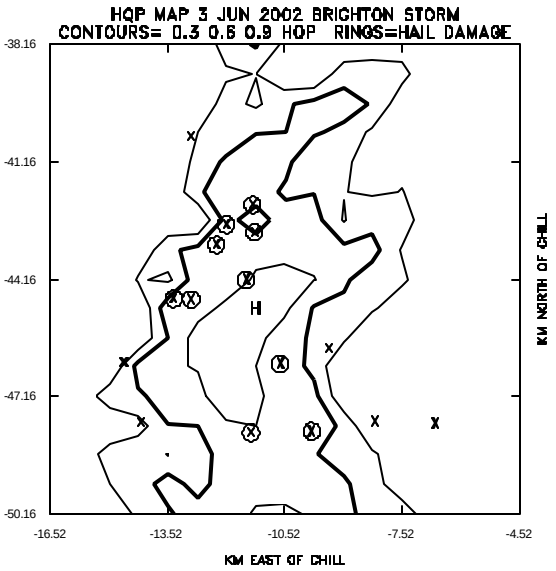

Figure 3: Example HQP map. Post storm damage survey data locations are shown with X's. Locations with documented structural hail damage are circled.

Figure 3 shows the resultant combination of an HQP-indicated hail swath and the observer data collected during post storm surveys. The hail was deposited by a pulse–type severe thunderstorm. Based on aerial video footage obtained by a television news helicopter, the hail completely covered the ground over a several square km area including point "H" (where the helicopter landed) in Fig. 3. The interviewed observers reported hailstones as large as golf balls (38 mm) and instances of structural damage. The patterns in figure 3 suggest that the reports of hail damage are correlated with the larger HQP magnitudes.

4. STATISTICAL ANALYSES

To support statistical testing of the hail characterization performance of both the HQP and HDR parameters, the basic PPI sweep input data were reprocessed such that a Cressman(1959) interpolation was centered on the GPS location associated with each ground verification point. The storm event maximum HQP and HDR values were then calculated at the ground observation locations.

The correlations between the HQP, HDR, and the post storm survey data were evaluated using statistical values based on the 2 x 2 contingency array method (Donaldson, et al., 1975, Doswell, et. al, 1990). Three verification conditions were tested: (1) Hail diameters of 19mm (.75 in) or larger, (2) Structural hail damage, and (3) The existence of hail of any diameter. (Structural hail damage was defined to be damage to building roofs, windows, siding, etc.) The performance of several polarimetric hail parameter values were tested against these verification conditions. The overall best performance for the discrimination of large / damaging hail was obtained by using an HQP threshold of 0.6 and HDR thresholds of 25 and 30 dB. The thresholds used for the detection of the existence of hail were 0.0 and 0.3 for HQP, and 0.0 dB for HDR.

All Cases

Size					
HQP 0.6		HDR 25		HDR 30	
POD:	0.673077	POD:	0.692308	POD:	0.480769
FAR:	0.204545	FAR:	0.2	FAR:	0.038462
CSI:	0.57377	CSI:	0.590164	CSI:	0.471698
HSS:	0.462069	HSS:	0.481865	HSS:	0.438127
TSS:	0.468531	TSS:	0.487762	TSS:	0.458042

Damage					
HQP 0.6		HDR 25		HDR 30	
POD:	0.923077	POD:	0.846154	POD:	0.769231
FAR:	0.314286	FAR:	0.352941	FAR:	0.130435
CSI:	0.648649	CSI:	0.578947	CSI:	0.689655
HSS:	0.628571	HSS:	0.539474	HSS:	0.717995
TSS:	0.673077	TSS:	0.573427	TSS:	0.701049

Any hail detection					
HQP 0		HQP 0.3		HDR 0	
POD:	0.850575	POD:	0.724138	POD:	0.942529
FAR:	0.038961	FAR:	0.015625	FAR:	0.046512
CSI:	0.822222	CSI:	0.715909	CSI:	0.901099
HSS:	0.345269	HSS:	0.285714	HSS:	0.474453
TSS:	0.517241	TSS:	0.613027	TSS:	0.498084

Four Largest Cases

Size					
HQP 0.6		HDR 25		HDR 30	
POD:	0.725	POD:	0.725	POD:	0.575
FAR:	0.064516	FAR:	0.147059	FAR:	0
CSI:	0.690476	CSI:	0.644444	CSI:	0.575
HSS:	0.527122	HSS:	0.391188	HSS:	0.446602
TSS:	0.607353	TSS:	0.430882	TSS:	0.575

Damage					
HQP 0.6		HDR 25		HDR 30	
POD:	0.92	POD:	0.84	POD:	0.76
FAR:	0.206897	FAR:	0.275862	FAR:	0.136364
CSI:	0.741935	CSI:	0.636364	CSI:	0.678571
HSS:	0.654412	HSS:	0.481618	HSS:	0.618575
TSS:	0.647273	TSS:	0.476364	TSS:	0.623636

Table 1: Statistical summaries of selected radar polarimetric radar hail parameter thresholds. POD: probability of detection, FAR false alarm ratio, CSI: critical success index, HSS: Heidke skill score, TSS:True skill score.

The verification performance is summarized in Table 1. The upper (all cases) portion of the table shows the results based on 96 ground survey size verification points and 70 damage verification points from 10 different storms. The tested polarimetric hail thresholds all show fairly good performance. The most accurate identification of 19mm or larger diameter hail was realized by the use of an HDR threshold of 25 dB. The best detection of verified structural damage due to hail was obtained with an HDR

threshold of 30 dB. The basic hail identification results vary among the statistical measurands; with the thresholds of HDR=0 dB and HQP=0.3 being similar. Thus, when the verification data from all of the surveyed hail events are considered, the additional information provided by the LDR component in the HQP calculation does not meaningfully improve the statistical performance indicies.

The lower portion of Table 1 shows the statistical results from the four storms that had two or more verifications of hail of 25mm (1 in) diameters or larger. For this hailstorm class, the HQP=0.6 threshold shows the greatest skill at identifying verification points where larger diameter hailstones and structural hail damage were confirmed. This implies that the LDR component in HQP may become more important with increasing hailstorm severity. As shown by the T-matrix modeling results, the causes of this behavior are complex. It is suspected that the increasing probability of somewhat rough, non-spherical hail shapes, coupled with Mie scattering resonance effects, may act to enhance the LDR levels in the more severe hailstorms.

5. SUMMARY

Based on the verification data collected in the COMET 2002 field project, it is apparent that the polarimetric (HDR and HQP) hail detection parameters are statistically superior to methods based only on Z_{hh}. For example, the analysis of WSR-88D reflectivity-based hail detection algorithms done by Kessinger and Brandes (1995) found maximum CSI values of .48 and Heidke skill scores of .36. The basic HDR hail parameter demonstrates considerable skill in the characterization of hail. As originally proposed by Aydin et al (1986), an HDR threshold of 0 dB is a useful indicator of the presence of hail in thunderstorm precipitation. Furthermore, the results of this study show that the HDR levels of 25 and 30 dB are indicative of hail diameters > 19 mm and structurally damaging hail respectively. It was only in storms where hail diameters > 25 mm were fairly commonly observed that the statistical performance of HQP exceeded that of HDR. The applicability of these results to other climatic regimes remains to be investigated.

For operational purposes, both HDR and HQP can readily be calculated and displayed in real time using individual PPI sweep input data. This permits the resultant diagnosed hail pattern depiction to be available before the completion of full radar volume scan. (As a part of the COMET project, color coded HQP field images were posted on the CSU-CHILL facility web page within ~1 minute of collection of the associated PPI sweep). A timely map presentation of accurately depicted hail fall areas is an improvement upon the use of a single numerical value (typically VIL (vertically integrated liquid)) to represent a thunderstorm's hail production characteristics. Also, additional research is necessary to determine if polarimetric radar observations of the upper portions of thunderstorms can improve the ability to anticipate the onset of hail at the ground.

Acknowledgements: Ms. Cathy Kessinger (NCAR) provided useful consultation on the statistical values in Table 1. Mr. Michael Silva, helicopter pilot for KCNC-TV in Denver Colorado, supplied video tape documentation of the hail deposition shown in Fig. 3. The CSU-CHILL facility is supported by NSF Cooperative Agreement ATM- 0118021. The COMET field project is funded by UCAR-COMET grant S02-38660.

6. REFERENCES

Aydin, K.., T. A. Seliga, and V. Balaji, 1986: Remote sensing of hail with a dual linear polarization radar. *J. Climate Appl. Meteor*., **25**, 1475-1484

Cifelli, R., D. Barjenbruch, D. Brunkow, L. Carey, C. Davey, N. Doesken, C. Gimmestad, T. Huse, P. Kennedy, and S. Rutledge, 2003: Evaluation of an operational polarimetric rainfall algorithm. Preprints, 31 Conf. on Radar Meteorology, Seattle, Washington

Cressman, G. P., 1959: An operational objective analysis scheme. *Mon. Wea. Rev.*, **121**, 2511-2528.

Donaldson, R. J., R. M. Dyer, and T. M. Kraus, 1975: An objective evaluator of techniques for predicting severe weather events. Preprints, 9th Conf. on Severe Local Storms, Norman, OK, Amer. Meteor. Soc., 321-326.

Doswell, C. A., III, R. Davies-Jones, and D. L. Keller, 1990: On summary measures of skill in rare event forecasting based on contingency tables. *Weather and Forecasting*, **5**, 576-585.

Husson, D., and Y. Pointin, 1989: Quantitative estimation of hailfall intensity with dual polarization radar and a hailpad network. Preprints, 24th Conf. on Radar Meteorology, Tallahassee, FL., Amer. Meteor. Soc., 318-321.

Kennedy, P., V. N. Bringi, D. A. Brunkow, S. A. Rutledge, and N. J. Doesken, 2001: Hail characterization via the joint utilization of reflectivity, differential reflectivity, and linear depolarization ratio data. Preprints, 30th Conf. on Radar Meteorology, Munich, Germany, Amer. Meteor. Soc., 433-435.

Kessinger, C. and E. A. Brandes, 1995: A comparison of hail detection algorithms. NCAR project summary report

Knight, N., 1986: Hailstone shape factor and its relationship to radar interpretation of hail. *J. Climate Appl. Meteor*., **25**, 1956-1958.

Waterman, P. C., 1965: Matrix formulation of electromagnetic scattering. *Proc., IEEE*, 53, 805-812.